Hyperspectral image analysis by scale-orientation morphological profiles

Antonio Plaza*, Pablo Martínez, Rosa Pérez, Javier Plaza
Neural Networks and Signal Processing Group (GRNPS), Computer Science Department,
University of Extremadura, Avda. de la Universidad S/N, 10071 Cáceres, SPAIN.

ABSTRACT

Mathematical morphology is a classic nonlinear image processing technique that has been successfully applied to analysis and classification of remotely sensed grayscale image data. The extension of basic morphological operations (i.e. erosion and dilation) to multi/hyperspectral imagery is not straightforward. In our approach, we treat the data at each pixel as a vector and impose a partial ordering of vectors in the selected vector space, based on their spectral purity. As a result, basic morphological operations are defined by extension, allowing joint spatial/spectral analysis of remotely sensed multispectral data. In this paper, we introduce the concept of scale-orientation morphological profile, and explore its application to mixed-pixel analysis and classification of hyperspectral data. The effectiveness of the proposed approach is assessed by using both simulated and real hyperspectral datasets collected by the NASA/Jet Propulsion Laboratory Airborne Visible-Infrared Imaging Spectrometer (AVIRIS). The proposed method is successfully applied for the purpose of land-cover classification and delineation of agricultural fields located at the Salinas Valley in California.

Keywords: Mathematical morphology, Extended morphological profiles, Spatial/spectral analysis.

1. INTRODUCTION

The integration of spatial/spectral responses in hyperspectral data analysis has been identified as a requested objective in the remote sensing community[1]. However, most available attempts are based on an initial clustering, using spectral information alone, followed by a post-classification step using spatial context. This operation entirely separates spatial information from spectral information, and thus the two types of information are not treated simultaneously. In previous work[2,3,4], we have explored the application of mathematical morphology operations to integrate both spatial and spectral responses in hyperspectral data analysis. Mathematical morphology[5] is a classic nonlinear image processing technique that has been successfully applied to the processing of remotely sensed imagery[1]. Based on the set theory, binary morphology was established by introducing fundamental operators applied to two sets[5]. One set is processed by another one having a carefully selected shape and size, and known as the Structuring Element (SE), which is translated over the image. The SE acts as a probe for extracting or suppressing specific structures of the image objects, checking that each position of the SE fits within the image objects. Morphological operations have extended to gray-tone (mono-channel) images by viewing these data as an imaginary topographic relief; in this regard, the brighter the gray tone, the higher the corresponding elevation[1]. It follows that, in grayscale morphology, each 2-D gray tone image is viewed as if it were a digital elevation model (DEM). In practice, set operators directly generalize to gray-tone images.

The extension of the concepts of binary and grayscale morphology to multi/hyperspectral images is not straightforward. When such techniques are applied independently to each image channel (marginal morphology), there is a possibility for loss or corruption of information of the image due to the probability that new spectral constituents —not present in the original image— may be created as a result of processing image channels separately[6]. An alternative way to approach the problem of multi/hyperspectral morphology is to treat the data at each pixel as a vector. In order to define the basic morphological operations, a concept for a maximum (or minimum) is necessary, and thus it is important to define an appropriate arrangement of vectors in the selected vector space. A number of vector ordering schemes has been proposed, since there is no natural means of defining arrangement in N-D spaces. Several approaches have been suggested[2]: 1) In reduced ordering, a scalar parameter function is computed for each pixel of the image and the ordering is performed according to the resulting scalar values; 2) In partial ordering, the input multivariate samples are partitioned

* E-mail: aplaza@unex.es; Phone: +34 927257195; Fax: +34 927257203.

Image and Signal Processing for Remote Sensing IX, edited by Lorenzo Bruzzone, Proceedings of SPIE
Vol. 5238 (SPIE, Bellingham, WA, 2004) · 0277-786X/04/$15 · doi: 10.1117/12.511110

into smaller groups which are then ordered; 3) In conditional ordering the vectors are initially ordered according to the ordered values of their components, e.g. the first component. At the second step, vectors that have the same value for the first component are ordered according to the ordered values of another component, e.g. the second component, and so on. Our approach to this problem has been the definition of scalar vector ordering schemes based on the spectral purity of pixels[3]. First, a lattice structure is imposed onto N-D space by the definition of a spectral angle distance-based cumulative measure. Second, morphological operations are defined by extension. By means of extended morphological operations, a method for mixed pixel analysis of hyperspectral data has been developed[4].

In this work, we extend our custom-designed morphological approach for mixed pixel analysis by using traditional scale-orientation representations[7]. Scale-orientation profiles have been used before for the detection of blob-like and linear structures in grayscale images. These signatures provide a rich local gray-level description at a pixel level, which is robust and locally stationary. Given this description, standard statistical classification methods can be used. In this work, we use extended scale-orientation morphological profiles to decompose hyperspectral images into components corresponding to different scales and orientations. Such modeling is important for many applications, including terrain classification and material identification. In addition, the high number of spectral bands in hyperspectral imagery provides a large number of spatial/spectral correlations that can be exploited for data modeling using extended scale-orientation morphological profiles.

The remainder of the paper is organized as follows. Section 2 describes the approach followed for extension of classic morphological operations to hyperspectral imagery. In section 3, a framework for the calculation of scale-orientation morphological profiles in hyperspectral data is described, and a number of examples are provided. Section 4 presents an application of the proposed analysis approach for the purpose of land-cover classification and delineation of agricultural fields located at the Salinas Valley in California, using AVIRIS data collected at the site in 1998. Finally, conclusions and comments on plausible future research are stated in section 5.

2. EXTENDED MORPHOLOGICAL OPERATIONS

Our attention in this section focuses primarily on the development of a mechanism to extend morphological operations to hyperspectral image data. Section 2.1 provides an overview of classic morphological operations. Section 2.2 focuses on the proposed framework to achieve the above goal.

2.1. Classic mathematical morphology

The two basic operations of classic mathematical morphology are dilation and erosion. Following a usual notation[8], let us consider a grayscale image f, defined on a space E. Typically, E is the 2-D continuous space R^2 or the 2-D discrete space Z^2. In the following, we refer to morphological operations defined on the discrete space. The flat erosion of f by $B \subset Z^2$ is defined by the following expression[8],

$$(f \otimes B)(x, y) = \bigwedge_{(s,t) \in Z^2(B)} f(x+s, y+t), \qquad (x, y) \in Z^2, \tag{1}$$

where $Z^2(B)$ denotes the set of discrete spatial coordinates associated to pixels lying within the neighborhood defined by B and $\bigwedge$ denotes the minimum. On the other hand, the flat dilation of f by B is defined by

$$(f \oplus B)(x, y) = \bigvee_{(s,t) \in Z^2(B)} f(x-s, y-t), \qquad (x, y) \in Z^2, \tag{2}$$

where $\bigvee$ denotes the maximum. Using the same notation above, the composition

$$(f \circ B)(x, y) = [(f \otimes B) \oplus B](x, y), \qquad (x, y) \in Z^2, \tag{3}$$

yields a flat opening, an operator that is increasing, anti-extensive, and idempotent[8]. On the other hand, the composition

$$(f \bullet B)(x, y) = [(f \oplus B) \otimes B](x, y), \quad (x, y) \in Z^2. \tag{4}$$

is called a flat closing, an operator that is increasing, extensive, and idempotent. A morphological operator is called a morphological filter if it is increasing and idempotent[8]. It is a common practice to use opening and closing morphological filters in order to isolate bright (opening) and dark (closing) structures in grayscale images, where bright/dark means brighter/darker than the surrounding structures in the image.

2.2. Extension of morphological operations to hyperspectral images

In order to extend basic morphological operations to hyperspectral images, let us now consider an image $\boldsymbol{f}$, defined on the $N-D$ continuous space, where N is the number of spectral channels. An ordering relation can be imposed in the set of pixels lying within a flat SE, denoted by B, by defining metrics that calculate the cumulative distance between one particular pixel $\boldsymbol{f}(x, y)$, where $\boldsymbol{f}(x, y)$ denotes an $N-D$ vector at discrete spatial coordinates $(x, y) \in Z^2$, and every other pixel in the neighborhood given by B. Based on the previous considerations, flat extended dilation and flat extended erosion can be respectively defined as follows

$$(\boldsymbol{f} \oplus B)(x, y) = \arg\left\{ \bigwedge_{(s,t) \in Z^2(B)} \left[\sum_s \sum_t \mathbf{Dist}(\boldsymbol{f}(x, y), \boldsymbol{f}(x+s, y+t)) \right] \right\}, \quad (x, y) \in Z^2, \tag{5}$$

$$(\boldsymbol{f} \otimes B)(x, y) = \arg\left\{ \bigvee_{(s,t) \in Z^2(B)} \left[\sum_s \sum_t \mathbf{Dist}(\boldsymbol{f}(x, y), \boldsymbol{f}(x-s, y-t)) \right] \right\}, \quad (x, y) \in Z^2, \tag{6}$$

where **Dist** is a point-wise distance measure between two $N-D$ vectors. The choice of **Dist** is a key topic in the resulting ordering relation. This study has been presented in previous papers[2,3,4]. In this work, **Dist** refers to the SAD distance, one of the standard metrics in hyperspectral analysis. Our choice of SAD is mainly based on the fact that this distance is invariant to multiplicative scaling that may arise due to different illumination conditions and sensor observation angle[2]. It should be noted that the $\arg$ operator in (5) and (6) respectively selects the $N-D$ pixel vector that maximizes and minimizes the cumulative distance value between $\boldsymbol{f}(x, y)$ and its neighboring pixels according to B. Hence, the use of SAD as the standard distance metric allows us to impose a partial order relationship of the vectors within an SE in terms of their spectral purity.

3. SCALE-ORIENTATION MORPHOLOGICAL PROFILES FOR HYPERSPECTRAL ANALYSIS

Our main goal in this section is to incorporate the idea of multi-scale analysis into extended morphological transformations. As described in section 2, morphological filters are characterized by the size, shape and orientation of the considered SE. However, if the searched patterns do not have regular properties across the scene, an adaptative scheme is needed to ensure that the correct SE size and orientation is considered at each pixel[4]. This need consequently poses the problem of adequate parameter selection. As reported by Pesaresi and Benediktsson[9], SE size selection can be achieved by plotting the morphological filter output at each pixel against the value of a varying parameter. The resulting plot is called a morphological profile, where the varying parameter is the size of the SE. Simple derivative rules can be applied to morphological profiles in order to determine the most appropriate parameter value for each pixel[9]. In the following subsections, we provide illustrative examples of extended morphological profiles, constructed using extended morphological operations. First, extended profiles are introduced in scale-space. Next, a mechanism to incorporate orientation information to multi-scale analysis is presented. Finally, section 3.3 describes a new methodology for mixed pixel classification, based on scale-orientation morphological profiles. The general algorithm, input parameters, and implementation options are also discussed.

3.1. Extended morphological profiles

This section provides some examples illustrating the construction of extended morphological profiles[6]. In Fig. 1, the construction of extended morphological profiles is illustrated by using four target objects in a hyperspectral image collected by the ROSIS imaging spectrometer over a semi-arid area in Cáceres, Spain: a small cork-oak tree [see Fig. 1(a)], a pure soil area [Fig. 1(b)], a medium-sized cork-oak tree [Fig. 1(c)], and a mixed area formed by soil and pasture, surrounded by pure soil [Fig. 1(d)]. Ground-truth information, collected during a site visit to the area, was used to characterize the spectral purity of sample pixels associated to these objects. As part of our experiment, the data from this site visit were compiled as a collection of spectral measurements with accurate geo-registration. Data collection revealed that, while the pixels in Figs. 1(a-c) can be considered spectrally pure, the relatively high spatial resolution available was not large enough to separate soil from pasture at the pixel shown in Fig. 1(d). As a result, this pixel was labeled as spectrally mixed. Extended morphological profiles were constructed for the pixels shown in Fig. 1. The resulting opening and closing profiles were combined in $3-D$ plots, where the spectral signature of the analyzed pixel $\boldsymbol{f}(x, y)$, denoted by P in the plots, is shown along with the resulting spectral signatures obtained after applying a series of extended opening and closing operations using different SE sizes. A range of SE's was considered in experiments. The range was derived by being based on three iterations of the elementary eight-connected SE. These iterations were labeled in the plots as $Ok = (\boldsymbol{f} \circ B)^k (x, y)$ for the opening series, and $Ck = (\boldsymbol{f} \bullet B)^k (x, y)$ for the closing series, where $k = \{1, 2, 3\}$. As it can be observed in Figs. 1(a-c), pure pixels remain indifferent to the three closing-by-reconstruction iterations, but are replaced during the opening-by-reconstruction process. Similarly, it is shown in Fig. 1(d) that the mixed pixel remains indifferent to the three opening-by-reconstruction iterations, but is replaced in the closing series. The step of the opening/closing series iteration at which the pixel is replaced provides an intuitive idea of both the spectral purity of the pixel and the spatial distribution of the object in the scene.

3.2. Scale-orientation morphological profiles for hyperspectral image interpretation

An extended scale-orientation morphological profile is defined as a tool to analyze the local neighborhood around a given pixel in terms of both spectral and spatial (with emphasis on scale and orientation features) information. Extended morphological operations are used to generate the scale-orientation space. A series of filtering techniques, based on selectively removing values in scale-orientation space, have been developed. The scale-orientation profile can be seen as a 2-D array where the rows represent scale and the columns represent orientation. The values in each column denote the change in spectral angle, resulting from applying morphological opening/closing series with SE's of varying size. On other hand, the values in each row are related to multiple orientations of line segment SE's centered at the pixel[10]. Scale-orientation morphological profiles can be graphically represented by gray-level maps. For illustrative purposes, Fig. 2 shows profiles taken from the centers of two target objects in a ROSIS hyperspectral scene: a tree and a linear feature. The profiles display uniform scale over orientation (for the tree) and varying scale over orientation (for the linear feature). It should be noted that the profiles shown in Fig. 2 have been generated for 12 orientations (from 0º to 180º) and 10 scales (from a 3x3-pixel SE to a 21x21-pixel SE).

3.3. Mixed-pixel analysis of hyperspectral imagery using scale-orientation morphological profiles

In this section, we describe the fundamentals a new algorithm for interpretation of mixed pixels in hyperspectral imagery, which makes use of scale-orientation morphological profiles. Taking into account the reasoning illustrated in sections 3.1 and 3.2, we can summarize the underlying ideas governing the algorithm as follows. Firstly, those pixels that remain indifferent to a closing series but are replaced during an opening series can be designed as "pure". In contrast, those pixels that remain indifferent to an opening series, but are replaced during a closing series, can be labeled as "mixed". Hence, pure/mixed pixels can be easily discriminated by comparing the maximum derivative value obtained in the opening series with the maximum derivative value produced by closing series. As previously reported[2], an initial labeling of pixels as "pure" instances may require an additional refinement, which in our case is developed using a region-growing process[4]. In this work, we have refined the region-growing procedure above by taking into account the information provided by scale-orientation morphological profiles. For each pixel, a neighborhood of interest is defined based on the maximum value of the scale-orientation profile, which provides an indication of the size and shape of the object that has been qualified as a "pure spectral constituent". The pixels in the area of interest are analyzed in terms of their spectral similarity to the originally selected pixel. Using this object-oriented approach, an endmember is selected for each "object", where an "object" may be defined as a spatially and spectrally coherent region in the scene, by using the following approach:

1. Original hyperspectral pixels labeled as "pure" instances are first selected as representative spectral signatures objects in the scene. These spectral signatures are considered as seed endmembers for each object.
2. Spatial neighbors are incorporated to each originally selected pixel if they are similar enough (cosine of spectral angle below 0.01) to the seed endmember, thus creating a bundle of spectral signatures, which are representative of the object. The spatial neighborhood analyzed is constructed by looking at the maximum value stored in the scale-orientation morphological profile associated to the pixel.
3. When no suitable neighbors can be incorporated in the bundle, the region growing process finishes and the median spectrum of the bundle is selected as a final endmember associated to the object.

Once a collection of representative spectral signatures have been selected for the pure areas in the scene, standard methodologies, such as linear/nonlinear mixture-based approaches, can be used to interpret the mixed pixels in the scene in terms of pure spectral signatures. The above procedure uses a scale-orientation morphological process to characterize pure spectral features in a given spatial domain range, and may be used to evaluate hyperspectral image pixels using a joint spatial/spectral criterion. The above criterion is used in this work for enhanced endmember selection.

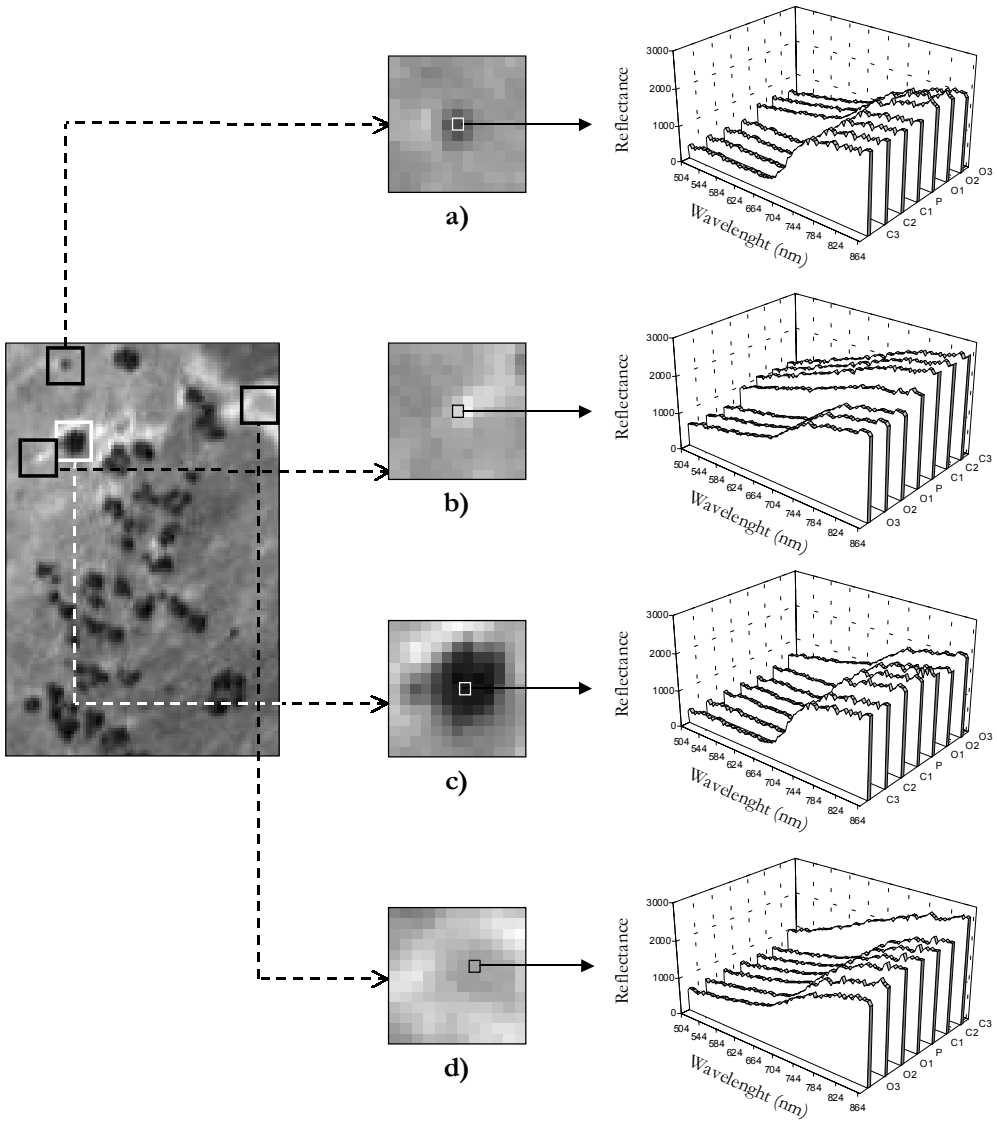

Figure 1. Extended morphological profiles associated to pixels belonging to four target objects in a ROSIS hyperspectral scene: (a) Small cork-oak tree, (b) Pure soil area, (c) Medium-sized cork-oak tree, (d) Mixed area formed by soil and pasture, surrounded by pure soil.

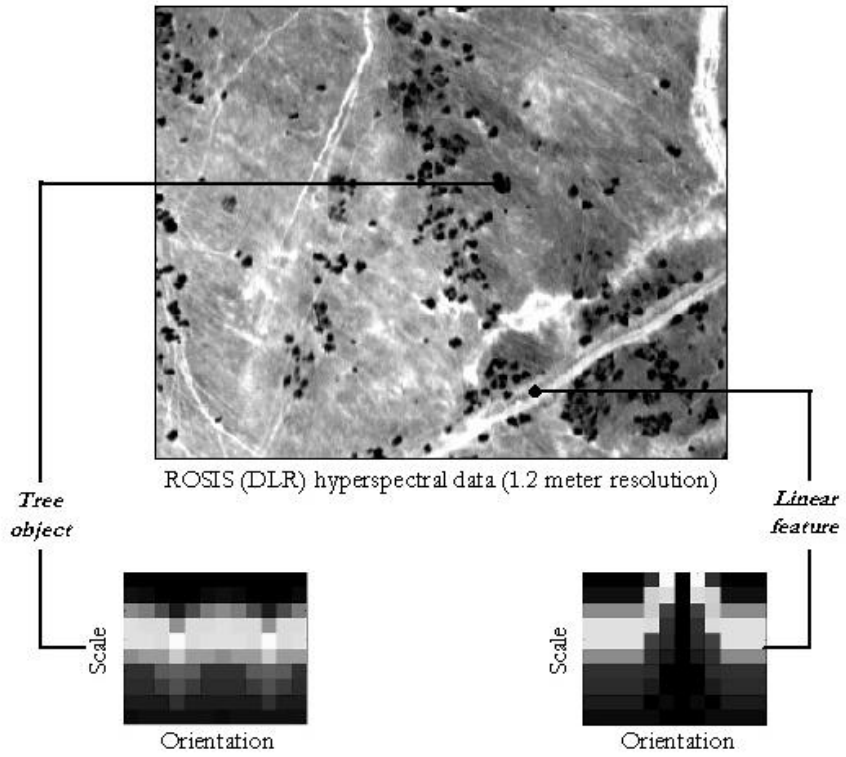

Figure 2. Scale-orientation morphological profiles taken from the centers of two target objects in a ROSIS hyperspectral scene: a tree (left) and a linear feature (right).

4. EXPERIMENTAL RESULTS

We have applied the mixed-pixel classification algorithm described in section 3.3 to real hyperspectral data collected by the AVIRIS imaging spectrometer in 1998 over Salinas Valley, California. The full scene consists of 512 lines by 217 samples with 224 spectral bands from 400 nm – 2500 nm with a pixel resolution of 3.7mx3.7m. These data was available only as at-sensor radiance data and includes vegetables, bare soils and vineyard fields. Fig. 3 shows the entire scene, along with ground-truth regions overlaid. We have selected a subscene of the Salinas 98 dataset called Salinas A, which comprises 83x86 pixels and includes six classes. Ground truth is available for most of the agricultural fields in this image, as described in Fig. 3. The spatial/spectral characteristics of the Salinas A dataset make it particularly suitable for testing the accuracy of our method. In particular, ground truth information reveals zones where broccoli with weeds, senesced corn and romaine lettuce are present. The romaine lettuce is at different weeks since planting (from 4 to 7) and with growth increasingly covering the soil.

With no availability of ground-truth information about the contribution of underlying constituent materials at each pixel in the above two scenes, a quantitative analysis for mixed pixel classification is not possible in this example. Hence, in order to carry out an experimental comparison between our mixed pixel classification algorithm and available ground-truth, it is first necessary to establish a link between mixed pixel classification and full pixel classification. In order to achieve such a goal, we follow an approach based on the definition of a mixed-to-pure (M/P) pixel converter[11]. This approach interprets the mixed pixel classification problem in the context of pure pixel classification by using the linear mixture model. Let us assume that the proposed mixed pixel classifier recognizes E pure signatures $\{\boldsymbol{e}_i\}_{i=1}^{E}$ in the scene, where $\boldsymbol{e}_j$ is the j-th signature. Let $\boldsymbol{f}(x,y)$ be a mixed pixel to be classified, and let $\hat{\alpha}(x,y)=[\hat{\alpha}_1(x,y)\hat{\alpha}_2(x,y)...\hat{\alpha}_E(x,y)]^T$ be the estimated E-dimensional abundance vector, where $\hat{\alpha}_j(x,y)$ is the estimated abundance fraction of material $\boldsymbol{e}_j$ in $\boldsymbol{f}(x,y)$. A simple M/P converter for $\boldsymbol{f}(x,y)$ can be constructed by using

the winner-take-all (WTA) thresholding criterion, an approach that is very similar to the WTA learning algorithm commonly applied in neural networks[11]. By using WTA, we can compare all estimated abundance fractions $\{\hat{\alpha}_1(x,y), \hat{\alpha}_2(x,y), ..., \hat{\alpha}_E(x,y)\}$ and find the one with the maximum fraction, say $\hat{\alpha}_{j^*}(x,y)$, by the following expression

$$j^* = \arg\left\{\max_{1\le j\le E}\{\hat{\alpha}_j(x,y)\}\right\}. \quad (7)$$

The resulting fraction is used to classify $\boldsymbol{f}(x,y)$ by assigning it to a class given by the j^*-th signature $\boldsymbol{e}_j$. In other words, using the WTA criterion we can define an M/P converter by setting $\hat{\alpha}_{j^*}(x,y)=1$ and $\hat{\alpha}_j(x,y)=0$ for $j\neq j^*$. With the above assumptions in mind, we proceed to describe in qualitative fashion the classification results obtained after applying our scale-orientation-based mixed pixel classifier to the Salinas C AVIRIS dataset. It should be noted that the range of scales and orientations used in this experiment consists of 12 orientations (from 0º to 180º) and 10 scales (from a 3x3-pixel SE to a 21x21-pixel SE). Fig. 4 shows the result obtained after applying the WTA M/P converter to the mixed pixel classification output provided by the proposed algorithm. A simple visual comparison of the classification image shown in Fig. 4 with ground truth in Fig. 3 reveals that the method is able to provide a smooth mapping of regions spatially. In addition, it can be seen that the method generates partitions that accurately represent structured directional regions in the image. These results can be attributed mainly to the adaptative selection of an optimum SE size and orientation for each pixel, which results in an optimization of the multi-scale morphological approach to endmember extraction. Overall, the proposed method works efficiently at both local and global scales, providing a final classification output that is coherent in both spectral and spatial terms in a complex, real-world scenario. Further quantitative results, using additional hyperspectral datasets with ground truth, are required in order to fully validate the proposed approach.

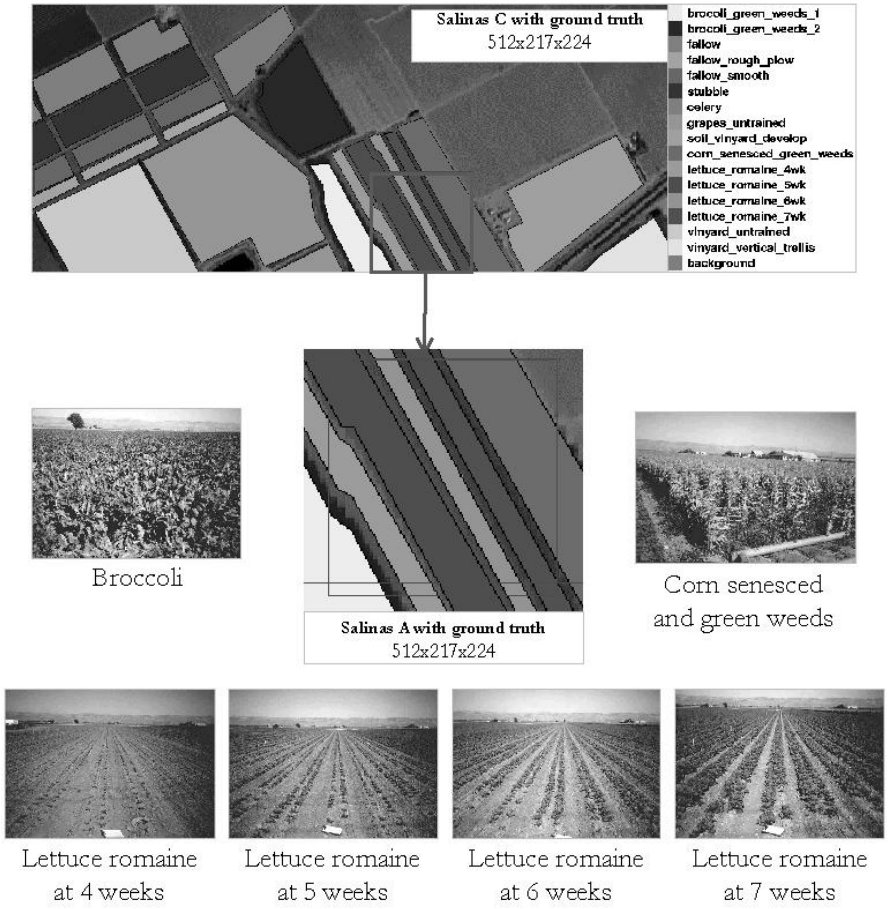

Figure 3. Salinas A and Salinas C AVIRIS data sets along with ground truth overlaid and pictures of several agricultural fields in the Salinas A subscene.

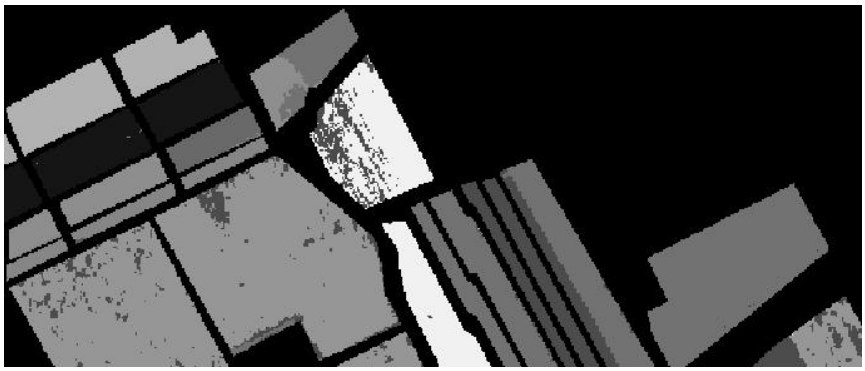

Figure 4. Classification image for AVIRIS Salinas C hyperspectral dataset, produced after applying the WTA M/P converter to the output provided by the proposed algorithm based on scale-orientation morphological profiles.

5. CONCLUSIONS AND FUTURE LINES

We have described a new morphological method for unsupervised mixed pixel classification in hyperspectral images. The method uses an adaptative approach, based on scale-orientation morphological profiles. This approach allows for the interpretation of each pixel of the scene by analyzing the spatial and spectral information in a combined manner. A preliminary evaluation of the proposed approach using real AVIRIS hyperspectral data over the Salinas Valley in California has been presented and discussed, revealing that the proposed method can be successfully applied for the purpose of land-cover classification and delineation of agricultural fields in a real scenario. A drawback of the proposed approach concerns the necessity of looking at a range of opening and closing operations with structuring elements of increasing size, which may result in a heavy computational burden when processing high-dimensional data. This phenomenon is particularly important in the case of images with large and homogeneous regions. In this regard, our current research focuses on the development of effective implementation strategies for the proposed approach. Massive parallel implementations using computer Beowulf-type cluster architectures are currently being investigated in order to empower the proposed methodology with near real-time capabilities.

REFERENCES

1. P. Soille and M. Pesaresi, "Advances in mathematical morphology applied to geoscience and remote sensing," *IEEE Transactions on Geoscience and Remote Sensing*, vol. 40, no. 9, pp. 2042-2055, Sept. 2002.
2. A. Plaza, P. Martínez, R. Pérez, J. Plaza, "Spatial/spectral endmember extraction by multidimensional morphological operations," *IEEE Trans. Geoscience and Remote Sensing*, vol. 40, no. 9, pp. 2025-2041, Sept. 2002.
3. A. Plaza, P. Martínez, J.A. Gualtieri, R. Pérez, "Spatial/spectral identification of endmembers from AVIRIS data using mathematical morphology," in: *X Airborne Earth Science Workshop*. Pasadena, CA, USA, 2001.
4. A. Plaza, P. Martínez, J.A. Gualtieri, R. Perez, "Automated identification of endmembers from hyperspectral images using mathematical morphology," in: *VIII SPIE International Symposium on Remote Sensing: Image and Signal Processing for Remote Sensing VII*. Toulouse, France, 2001.
5. J. Serra, *Image Analysis and Mathematical Morphology*. New York: Academic, 1982.
6. A. Plaza, P. Martínez, R. Pérez, J. Plaza, "A new method for target detection in hyperspectral imagery based on extended morphological profiles," in: *IEEE IGARSS*. Toulouse, France, 2003.
7. R. Zwiggelaar, C.J. Taylor, "Linear and non-linear modelling of scale-orientation signatures," in: *Proceedings of Non-Linear Model Based Image Analysis*, pp. 152-157, 1998.
8. P. Soille, *Morphological Image Analysis. Principles and Applications*. Springer Verlag, 2003.
9. M. Pesaresi and J. Benediktsson, "A new approach for the morphological segmentation of high resolution satellite imagery," *IEEE Trans. Geoscience and Remote Sensing*, vol. 39, no. , pp. 309-320, Feb. 2001.
10. P. Soille, H. Talbot, "Directional morphological filtering," *IEEE Trans. Pattern Analysis and Machine Intelligence*, vol. 23, no. 11, pp. 1313-1329, 2001.
11. C.-I Chang, H. Ren, "An experiment-based quantitative and comparative analysis of hyperspectral target detection and image classification algorithms," *IEEE Trans. Geoscience and Remote Sensing*, vol. 38, no. 2, pp. 1044-1063, 2000.